

# The mechanics of stretch-graphitization of glassy carbon fibres

H. M. HAWTHORNE\*

*Centre for Materials Research, The University of British Columbia, Vancouver, B.C., Canada*

The mechanics of stretch-graphitization of glassy carbon fibres made from two pitch precursors was studied by determining the plastic deformation characteristics of monofilaments during their elongation to 50% strain in a continuous apparatus. By monitoring fibre tension under various processing conditions and analysing deformation profiles quenched into extending fibres, the temperature and strain-rate dependence of induced fibre stresses has been obtained. Over the temperature range 2200 to 3000° C and strain-rate range  $3.0 \times 10^{-4}$  to  $2.5 \times 10^{-1} \text{ sec}^{-1}$ , tensile stresses in the glassy carbon fibres ranged from 7000 to 50 000 psi. The deformation can be described by the empirical equation  $\dot{\epsilon} = A \sigma^n \exp(-\Delta H/RT)$ , where  $A$  is a constant,  $n = 8.6 \pm 1$  and  $\Delta H \sim 290 \pm 50 \text{ kcal mole}^{-1}$ , independent of temperature and strain-rate, for both fibre types. The apparent activation energy is consistent with the controlling operation of a microfibrillar reorientation process, accompanied by atomic diffusion (ordering). The high strain-rate stress dependence, indicating an apparent activation volume  $\sim 4000 \text{ \AA}^3$ , also suggests a molecular-scale rate-limiting process. Results are compared with those of various high temperature processes in carbonaceous solids and deformation in organic polymers and it is suggested that stretch-graphitization can be considered analogous to the affine drawing of amorphous polymer fibres.

## 1 Introduction

The microstructure of glassy carbon fibres corresponds closely to that of other glassy carbon solids and, except for the much higher tensile strength of the filaments, their physical and mechanical properties are generally similar to those of the equivalent bulk material [1, 2]. Belonging to the class of polymeric carbons, these fibres are produced by the spinning and subsequent slow carbonization of precursors, such as thermoset resins [1, 2] and pitches [3], which can be cross-linked prior to carbonization. Oriented, high modulus carbon fibres can be made from the isotropic glassy carbon fibres by "stretch-graphitization" whereby the filaments are given a permanent extension at high temperatures [4, 5]. In its continuous form [4] this stretch-graphitization is essentially a strain-controlled, tensile plastic deformation process in

which stresses induced in the deforming fibres depend on the particular processing conditions applied.

The stretch-graphitization process has also been used to increase the axial preferred orientation texture, present to varying extents, in carbon fibres prepared from textile polymer fibres, notably rayon [6] and PAN [7]. However, although considerable information on the structure and property changes which result from such stretching has been reported for these [7-9] as well as for pitch-based filaments [4, 5, 10, 11], nothing has so far been published on the mechanics of the fibre deformation.

This paper describes a determination of the characteristic parameters of the high temperature plastic deformation taking place during the stretch-graphitization of glassy carbon fibres. The tem-

\* Present address: MacTainAir Systems Ltd, 420 Cowley Crescent, Vancouver Airport, Richmond, B.C., Canada.

perature and strain-rate dependence of tensile stresses have been obtained by monitoring the tension in monofilaments during their elongation to 50% strain in a continuous, laboratory scale, apparatus. Further information on process dynamics has been gained from analysis of deformation profiles quenched into deforming fibres. Results are discussed in relation to rearrangements of the fibre microstructure and comparison is made with corresponding data for various high temperature processes in bulk carbons and graphites and deformation in organic polymers. The term carbon fibre is used herein for all carbonaceous filaments irrespective of their microstructure or their process history.

## 2. Experimental

### 2.1. Materials

Glassy carbon monofilaments (Great Lakes Carbon Corp) made from coal-tar pitch or those prepared here (C.M.R. carbon fibres) from a highly aromatic, petroleum pitch were used. The former were either 24 or 55  $\mu\text{m}$  in diameter with nominal U.T.S. values of  $1.2 \times 10^5$  or  $0.95 \times 10^5$  psi\* respectively while the latter ranged between 20 and 60  $\mu\text{m}$  diameter and exhibited mean tensile strengths between 0.9 and  $1.3 \times 10^5$  psi. Both fibre types met the requirements of availability as long lengths, diameter uniformity and adequate and consistent tensile strengths. Also by using these large diameter fibres, sufficiently large filament tensions for their accurate measurement were obtained even for the lowest stresses induced during the stretching experiments.

### 2.2. Apparatus and procedures

A schematic illustration of the stretch-graphitization apparatus is shown in Fig. 1. The glassy carbon monofilaments were fed from the feed spool via a train of three light, low-friction pulleys through a small induction heated furnace and onto

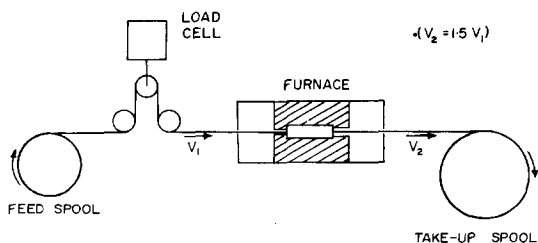


Figure 1 Schematic illustration of stretch graphitization apparatus.

\*  $10^3$  psi = 6.89 N mm<sup>-2</sup>.

the take-up spool. In operation both spools were driven at the same speed through a 250:1 reduction gear by a variable speed D.C. motor, the output of which could be precisely controlled. A constant extension of 50% was imposed on the continuously moving fibre by the 1.5:1 ratio of spool diameters. The graphite tube susceptor (0.25 in. o.d., 0.1 in. i.d., 2 in. long) was insulated from the surrounding vycor tube by graphite felt. Felt inserts also covered the furnace entrance, the fibre passing through a small hole in the felt while the exit was partially covered leaving a 0.1 in. diameter hole through which furnace interior temperatures were sighted. Susceptor and insulation were maintained in an argon atmosphere.

Furnace temperatures, measured with a newly calibrated, disappearing-filament optical pyrometer, were corrected using a graphite emissivity of 0.8 [12]. Fibre temperature was assumed to be the same as that of the furnace interior. This furnace maintained steady temperatures (within the limits of measurement) over the length of time required for experimental runs and was capable of relatively fast temperature response to changes made in the induction generator output. Tension in the moving fibre was monitored continuously, to an accuracy of  $\pm 0.05$  g, by means of an Instron type A load cell coupled to a strain gauge bridge and chart recorder. (The stability of this load sensing system under processing conditions was checked by driving fibre between equal diameter spools).

In the present experiments tensions were measured on fibres which were undergoing stretch-graphitization at a number of different rates, determined by the motor speed drive, and at various temperatures. Fibre stresses were calculated on the basis of initial cross-sectional areas, i.e. those of the glassy carbon fibres. Strain-rates corresponding to various motor speeds were calculated based on the average fibre velocity over the 2 in. length of furnace assuming all of the deformation occurred inside the furnace. The validity of this procedure was established in separate experiments by analysis of the velocity profiles along the furnace zone for fibres undergoing stretching at both fast and slow rates. By cutting deforming fibres at a fixed position they were rapidly ejected from the furnace by the line tension. The frozen-in diameter profiles thus obtained were examined at  $\frac{1}{8}$  in. intervals along the fibre length. A similar

quenching experiment was carried out to provide a more complete process profile by determining the sequential fibre structure and physical property variations thus giving further information on the deformation characteristics. Fibre diameters, densities and structure parameters were measured as before [10]. Young's modulus of the  $\frac{1}{8}$  in. long fibre pieces was determined by glueing them to a piezo-electric crystal and recording the fundamental mode

frequency of their flexural vibrations. Velocity and % deformation profiles were calculated assuming constant volume deformation conditions.

### 3. Results

#### 3.1. Quenched profiles

Some physical property and structural parameter profiles determined on a petroleum-pitch-based glassy carbon fibre being stretched to 100% elong-

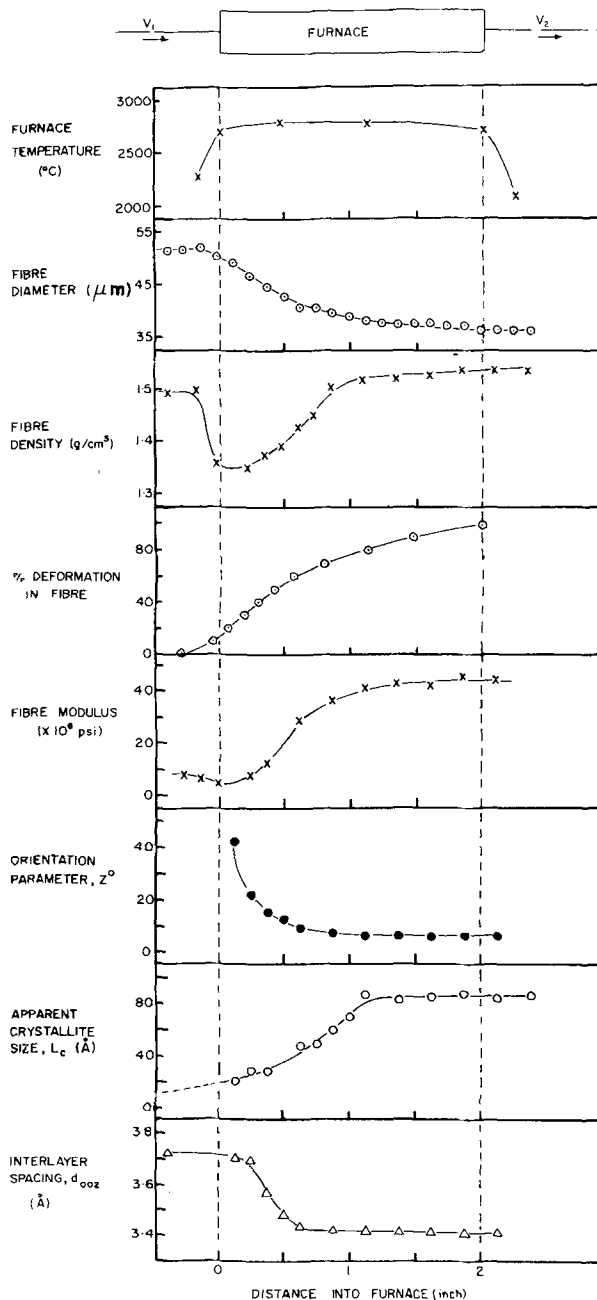


Figure 2 Property and structure parameter profiles in the deformation zone of a glassy carbon fibre undergoing stretching to 100% extension at  $\sim 2800^{\circ}\text{C}$ .

ation are presented in Fig. 2. Similar, though less pronounced, profiles are obtained at 50% extension but the higher elongation shows more clearly the sequential changes especially in fibre diameter, modulus and preferred orientation. Since the tension on this fibre during deformation at  $\sim 2.5$  g was relatively low, corresponding to an initial stress of  $\sim 16\,000$  psi, no appreciable viscoelastic relaxation distorts the quenched profiles. Under very high stress conditions (e.g. at low temperatures) such quenched-in relaxation effects are readily observed as a considerable increase in fibre diameter, relative to that of the glassy carbon fibre, in the region close to the furnace entrance.

Fig. 3 shows that there is little difference between fibre velocity profiles (calculated from diameter profiles) in the furnace for fast and slow processing rates on fibres being stretched to 50% elongation. Since average strain-rates over the furnace length were used to interpret results it is important to know that these bear the same relationship to the maximum strain-rates sustained by each fibre over the range of processing speeds applied in the stretching experiments. Similarly it can be shown that the flow stress profiles, which are inversely related to the diameter profiles, remain essentially constant.

### 3.2. Strain-rate and temperature dependence of the fibre tension

Fig. 4 shows typical variations in fibre tension (traced from original recordings with the ordinate

scale divided by two) for fibres deforming under several applied average strain-rates at two different temperatures. After large strain-rate changes transient load values were often obtained, especially upon reducing the processing speed. Loads lay within the range 3 to 20 g and were monitored for a sufficient time at each rate to record the equilibrium values, which usually remained constant over long time periods. As can be seen from Fig. 4, largest load changes for a given strain-rate change were observed at low temperatures.

Strain-rate change experiments were carried out over the temperature range 2250 to 3000° C with average strain-rate ranges of  $3 \times 10^{-4}$  to  $2.5 \times 10^{-1}$  sec<sup>-1</sup> at high temperatures and  $3 \times 10^{-4}$  to  $2.8 \times 10^{-2}$  sec<sup>-1</sup> at the lower temperatures. In some experiments, changes in strain-rate were made between several high rates and also between several low rates to sensitively check for any dependence of the strain-rate – fibre tension relationship on strain-rate.

The variation of tension in deforming monofilaments with temperature at constant applied strain-rate is illustrated by the typical recording in Fig. 5. The length of time required to establish equilibrium conditions was greatest for changes to low furnace temperatures, reflecting the slower response to cooling of the well insulated susceptor, but the recorded loads eventually became constant. Temperature change experiments were performed at several constant strain rates and over the temperature range 2150 to 3000° C. Any possible effect

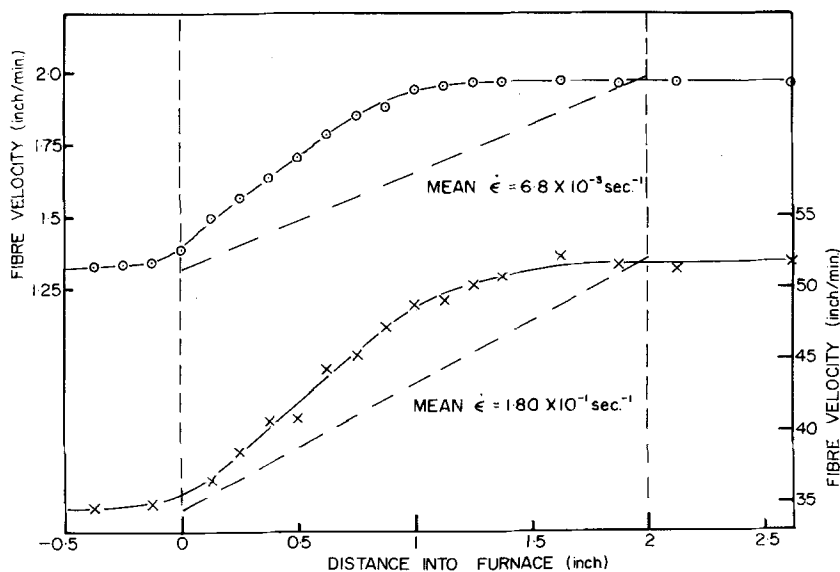


Figure 3 Fibre velocity profiles for a fibre being stretched to 50% extension at fast and slow processing speeds showing approximate constancy of profiles and their relationship to average velocities (dashed lines) over the furnace zone.

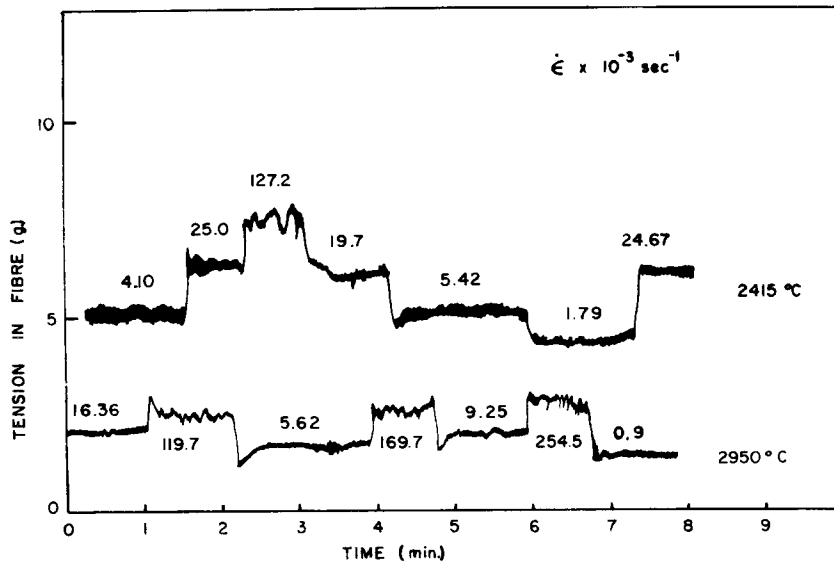


Figure 4 Portions of typical fibre tension ( $\frac{1}{2}$  recorded load) versus time recordings for fibres being stretch-graphitized showing effect of (average) strain-rate changes at two different temperatures.

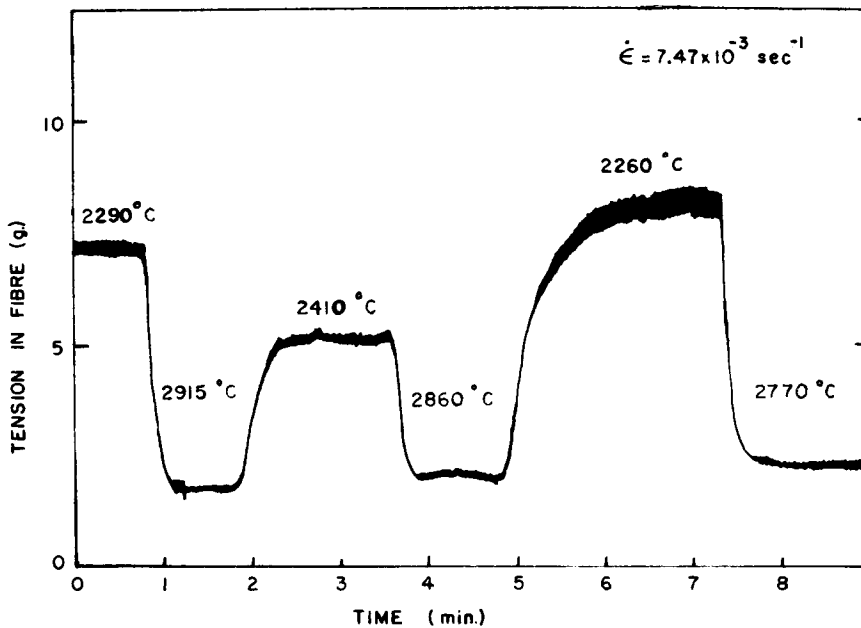


Figure 5 Fibre tension versus time recordings for a fibre being stretch-graphitized at a fixed (average) strain-rate showing effect of temperature changes.

of temperature on the temperature–tension dependence was directly examined in a similar way to that described for the strain-rate change experiments.

In the stretch-graphitization experiments the thickness of recorded traces, which varied with the size of the load, was due to the existence of small but real sawtooth oscillations in the actual fibre

tension. These oscillations are clearly resolved in very low strain-rate experiments as shown in Fig. 6. Investigation showed that these small oscillations increased in frequency with both increasing temperature or applied strain-rate and that they were not due to any artefact of the stretching apparatus or load measuring system.

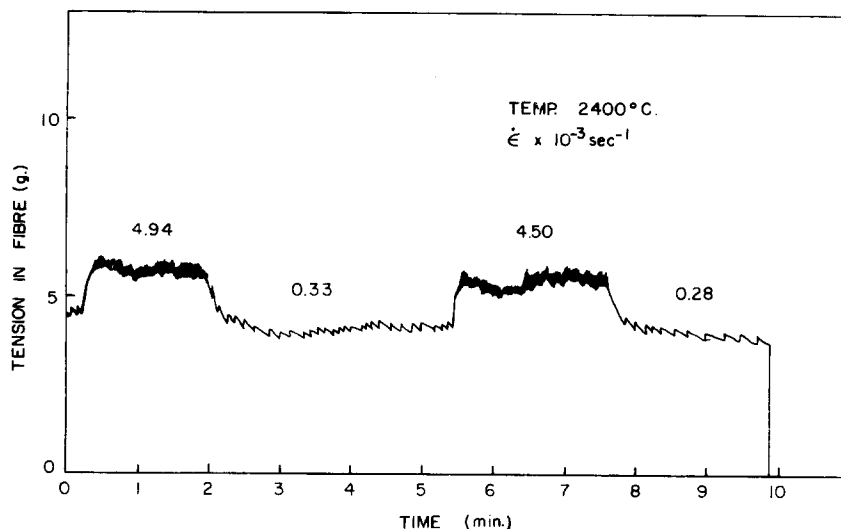


Figure 6 Fibre tension versus time recordings for a fibre being stretch-graphitized at low strain-rates showing resolution of small sawtooth oscillations which are always present during stretching.

### 3.3. Interpretation of results

In the stretch-graphitization of all glassy carbon fibres, at least for moderate extensions, the ratio of the cross-sectional areas of stretched and undeformed fibres lies close to what would be expected on the basis of constant volume deformation. This is illustrated by the diameter profile shown for the petroleum-pitch-based fibres in Fig. 2. It is also seen from Fig. 2 that the assumption that all the deformation occurs within the 2 in. furnace length is a reasonable approximation. In any case, since the mean strain rates calculated based on this 2 in. length are shown in Fig. 3 to bear essentially the same relationship to the maximum strain-rates sustained by the fibres at both fast and slow processing speeds (Maximum rates  $\sim 1.2 \times$  mean rates), this assumption is not important. Although deformation stresses will be dependent on the maximum strain-rates in the extending fibres, because of this constant relationship the same stress-strain-rate dependence will result from use of the average rates in the following treatment of results.

When a constant tension is monitored in the system the flow stress existing in any increment of the deforming fibre is inversely related to the instantaneous fibre diameter at that point. Since the diameter profile remains substantially constant over the range of processing conditions applied, the variation (with temperature or strain-rate) in the stress level at any position along the fibre can be used to ascertain the stress-temperature and

stress-strain-rate relationships inherent in the stretch-graphitization process. For convenience, representative deformation stresses are obtained based on the glassy carbon fibre diameter.

The microstructures and physical properties of stretch-graphitized glassy carbon fibres are not very sensitive to changes in processing rates over the ranges studied but, as has been shown previously [10], for a given fibre and extension there is some dependence on temperature, of those parameters related to the extent of structural ordering (see Section 4.2) in the fibre. However, in relation to the overall changes from the initial ( $1000^\circ\text{C}$ ) glassy carbon state, consequent upon the stretch-graphitization these variations are small and it is assumed for the present that essentially the same processes operate in the fibres over the experimental range of conditions presently applied.

These stretch-graphitization experiments, where fibres are plastically deformed in a dynamic, but effectively steady-state, system between about 0.6 to  $0.85 T_m$ , are somewhat analogous to high temperature, differential constant strain-rate tensile tests, in that tensile flow stresses are obtained as a function of strain-rate at constant temperature or of temperature at constant strain-rate. The formalism for analysis of such tensile test results is, therefore, adopted here for interpretation of present data.

In Fig. 7 fibre stresses are plotted against applied mean strain-rates for two typical strain-rate change experiments. From the reasonably

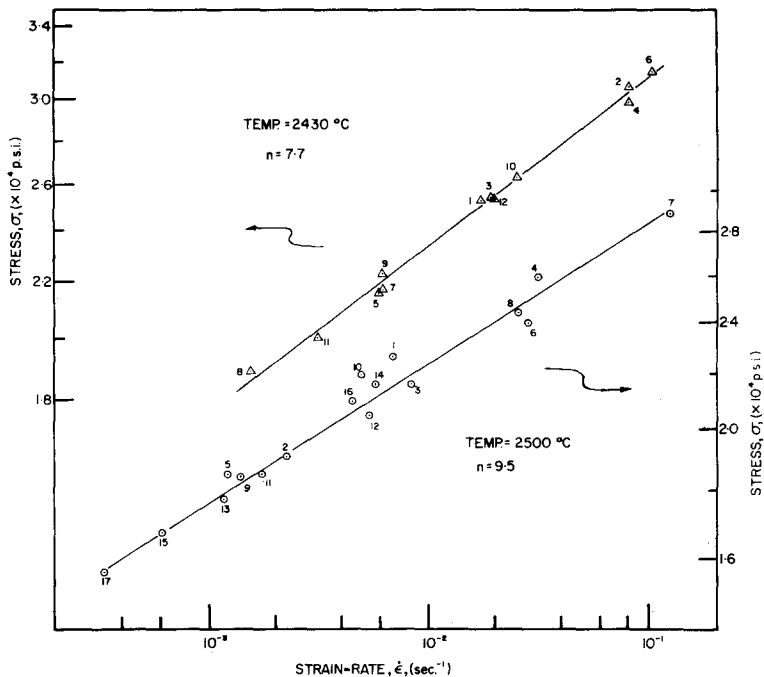


Figure 7 Variation of fibre tensile stress with applied (average) strain-rate for two typical strain-rate change experiments. Numbers beside plotted points show order in which strain-rate changes were made. (Fibre stresses calculated based on glassy carbon fibre diameter – see text).

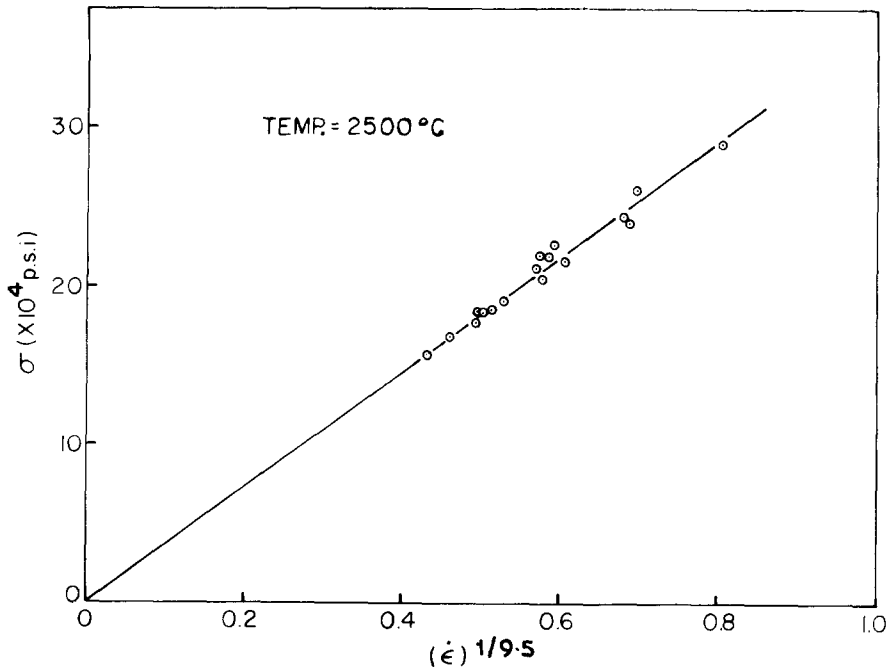


Figure 8 Fibre stress versus  $1/9.5$  power of the strain-rate for one set of data from Fig. 7, showing that the best line through plotted points extrapolates to the origin.

good fit of these results and all similar data, to a linear relationship on such plots it appears that the stress is related to strain-rate by a power law over the strain-rate ranges investigated. This may be

expressed by the equation

$$\sigma = (\dot{\epsilon})^{1/n} + c$$

where  $\sigma$  is the tensile stress,  $\dot{\epsilon}$  is the mean strain-

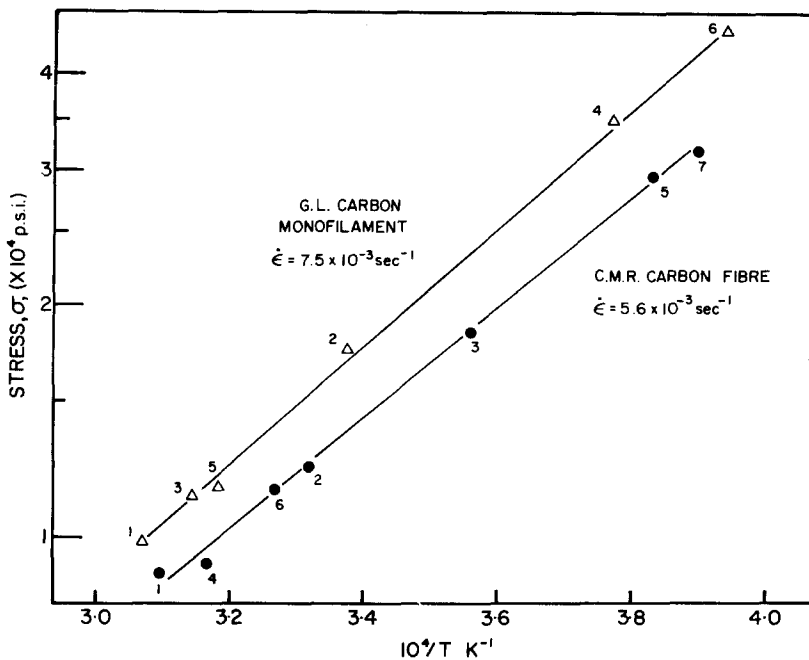


Figure 9 Variation of fibre tensile stress with temperature for two typical temperature change experiments. Numbers at points show order in which data were taken.

TABLE I Stress exponents and apparent activation energies for deformation of glassy carbon fibres

	Petroleum-pitch-based (C.M.R.) fibre	Coal-tar-pitch-based (G.L.) fibre
$n = \frac{d \log \dot{\epsilon}}{d \log \sigma}$	8.8	8.1
	7.8	8.7
	8.1	9.1
	8.0	7.7
	9.3	10.7
	9.0	8.9
	8.4	9.5
	—	7.1
Means	$8.48 \pm 0.6$	$8.71 \pm 1$
Combined mean $n = 8.6 \pm 1$		
$\Delta H = nR \frac{d \ln \sigma}{d(1/T)}$ ( $n = 8.6$ )	298.4	283.6
	286	289
	273.4	307.5
	283.6	297.8
	256.3	310.5
	273.4	309.3
	307	306
	Means	$282.6 \pm 16.9$
Mean $\Delta H$ using $n = 8.6 \pm 1$	$282.6 \pm 49.3$	$300.5 \pm 45.6$
Combined mean $\Delta H \sim 292 \pm 48 \text{ kcal mol}^{-1}$		



rate,  $n$  is the stress exponent and  $c$  a constant. For one particular set of results in Fig. 7,  $n = 9.5$ . These results are replotted as  $\sigma$  versus  $(\dot{\epsilon})^{1/9.5}$  in Fig. 8 in which the best line through the plotted points extrapolates to the origin, indicating  $c = 0$ . Corresponding treatment of the data from the other strain-rate change experiments similarly indicates the absence of an athermal component in the flow stress. The stress exponents from all experimental runs on both types of glassy carbon fibres are listed in Table I.

Fig. 9 shows examples of results from temperature change experiments for one representative determination from each of the two fibre types. From the linearity of all such plots and those of Figs. 7 and 8 an empirical equation describing the fibre deformation can be written as

$$\dot{\epsilon} = A\sigma^n \exp(-\Delta H/RT)$$

where  $A$  is a constant,  $\Delta H$  is the apparent activation energy of the rate-limiting deformation process and  $R$  and  $T$  have their usual meaning. The various  $\Delta H$  values calculated from all Fig. 9 type plots, using the combined mean  $n$  value of 8.6 for the two glassy carbon fibres, are listed in Table I. No correlation between either  $\Delta H$  or  $n$  and temperature or strain rate was apparent over the ranges studied which supports the assumption of little variation in fibre processes over the range of experimental stretch-graphitizing conditions.

The difference between the two mean  $n$  values for the two fibre types is not significant. That between the two mean  $\Delta H$  values is statistically significant at the 95% confidence level ( $t$ -test).

However, since furnace temperatures measured by the optical pyrometer are, at best, accurate only to  $\sim \pm 10^\circ \text{C}$ , uncertainty in individually determined  $\Delta H$  values could be at least  $\pm 30 \text{ kcal mol}^{-1}$  [13], so this apparent difference between average results for the two different glassy carbon fibres is open to some doubt. A combined mean  $\Delta H$  value of  $292 \pm 48 \text{ kcal mol}^{-1}$  is, therefore, included in Table I as the effective activation energy for the stretch-graphitization of all the glassy carbon fibres.

## 4. Discussion

### 4.1. Comparison with various high temperature processes in carbons and graphites

A comparison of some representative results from the stretch-graphitization of the glassy carbon fibres with those obtained from creep testing of bulk glassy carbons [14] is shown in Fig. 10. These plots of the data from two quite different experiments match well in their stress-strain-rate relationship. While the stress exponents obtained from the creep experiments varied with stress [14], the data trend, as seen in Fig. 10, suggests an approach to a constant value ( $n \geq 6.5$ ) at the higher strain-rates. This is consistent with the average value of 8.6 obtained for the fibre deformation. The lower stress levels of present data, compared with the creep data (extrapolated to corresponding strain-rates) may indicate the relative ease of deforming the two differently heat-treated carbons (see Section 4.2) but they also reflect the fact that fibre stresses were calculated based on their initial cross-section areas. Any adjustment for strain

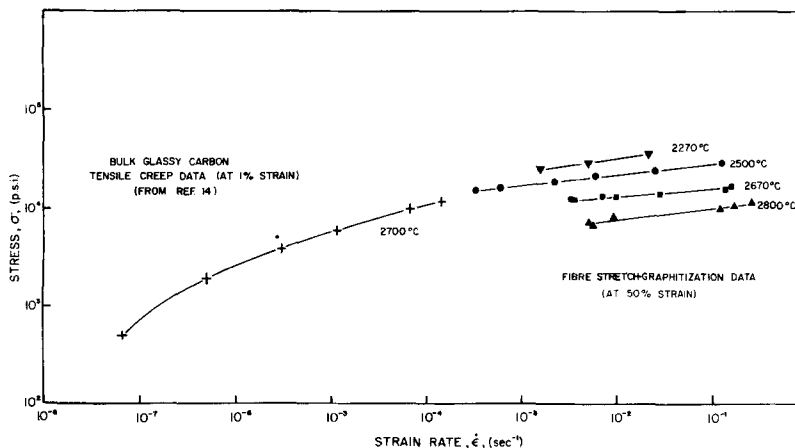


Figure 10 Comparison of stress-strain-rate data from creep experiments on bulk glassy carbon with some typical glassy carbon fibre stretch-graphitization data.

TABLE II Comparison of apparent activation energies for high temperature deformation and graphitization and stress exponents for deformation in various carbons and graphites

Material	Experiment	$\Delta H$ (kcal mol <sup>-1</sup> )	$n$ (stress range, 10 <sup>3</sup> psi)	Reference
Glassy carbon	Stretch-graphitization	$\sim 290 \pm 50$	$8.6 \pm 1$ (7–50)	This work
Bulk glassy carbon	Tensile creep	$\sim 350 \pm 45$	1.5 – 6.5 (6–16)	[14]
Pyrolytic carbon	Basal shear	$\sim 270$	3	[34]
Pyrolytic carbon	Creep	$\sim 250 \pm 40$	4 (< 1% strain) 1.5 (> 4% strain)	[15]
Binder/filler graphite	Creep	$\sim 250 \pm 20$	6–8 (4–5)	[35]
Poco graphite	Creep	$\sim 230 \pm 30$	5 (6–9)	[35]
Poco graphite (annealed 2900° C)	Creep	$\sim 250 \pm 20$	8 (6–9)	[35]
Pyrolytic carbon	Graphitization	$\sim 260$	–	[15]
Binder/filler graphite	Graphitization	$\sim 260$	–	[15]
Cokes	Graphitization	$\sim 230 \pm 15$	–	[36]
Carbon fibre/C.V.D. matrix composites	Graphitization	{(a) $240 \pm 35$ (b) $276 \pm 28$	–	[37]

differences between the two experiments would shift the (extrapolated) creep data to even larger stresses because of creep hardening effects [14].

In Table II the average apparent activation energy and stress exponent found for the stretch-graphitization of glassy carbon fibres are listed along with corresponding reported data for high temperature deformation and activation energies for graphitization (a structure change process) in several carbons and graphites. The present stress exponent is about the same as the highest values reported in several solids, which were mostly studied at lower stresses. At  $\sim 290$  kcal mol<sup>-1</sup>, the present mean  $\Delta H$  value lies between that reported for creep in bulk, high temperature heat-treated, glassy carbon and the average value for graphitization (and high temperature deformation) in most other carbonaceous solids. As discussed further in Section 4.2, this is consistent with structural ordering and plastic deformation processes operating simultaneously and interactively during the stretch-graphitization treatments.

If real, the slight difference between  $\Delta H$  values for the two types of glassy carbon fibre might be due to initial microstructural variations (e.g. in cross-link density) such that the interaction between the deformation and graphitization processes differed in each case. Although considerable disparity in the ease of stretch-graphitizing these two fibre types, particularly at extensions >100%, has been noted previously [16], no detailed comparative analysis of microstructure and/or composition of these fibres has been made. The above must, therefore, remain speculative at present, and the effective activation energy for stretch-

graphitization of all glassy carbon fibres is taken as the combined mean value as in Table II.

#### 4.2. Mechanism of stretch-graphitization

There is considerable controversy over some aspects of bonding and microstructure in glassy carbons [1, 2, 17–21]. Dispute is mainly concerned with the existence of carbon atoms in bonding states other than sp<sup>2</sup> hybridization and a variety of models have been proposed for the detailed glassy carbon structure [1, 2, 17, 20]. It is mostly agreed, however, that the majority of the carbon atoms exist in the trigonal configuration in narrow, often distorted, graphite-like layers or ribbons, imperfectly stacked (turbostratic graphite) in groups which form a randomly interlinked, three dimensional network [2, 17–20]. This branched ribbon, or microfibrillar substructure model was initially proposed to represent the structure of oriented carbon fibres [22] which, it was later reported [4, 5, 10], could be made from isotropic glassy carbon fibres by hot-stretching. This model was, therefore, adopted for the glassy carbon structure when it was shown [2] that the wrinkled and twisted ribbon units, which were more or less axially aligned in the fibres, were randomly oriented and more disordered (to a degree dependent on their heat-treatment) in the isotropic material.

The two main effects of the high temperature plastic deformation applied to the present (1000° C) glassy carbon fibres during their stretch-graphitization are thus a marked structural ordering of the distortions and defects, both in layer stacking and within the layers and of any inter-

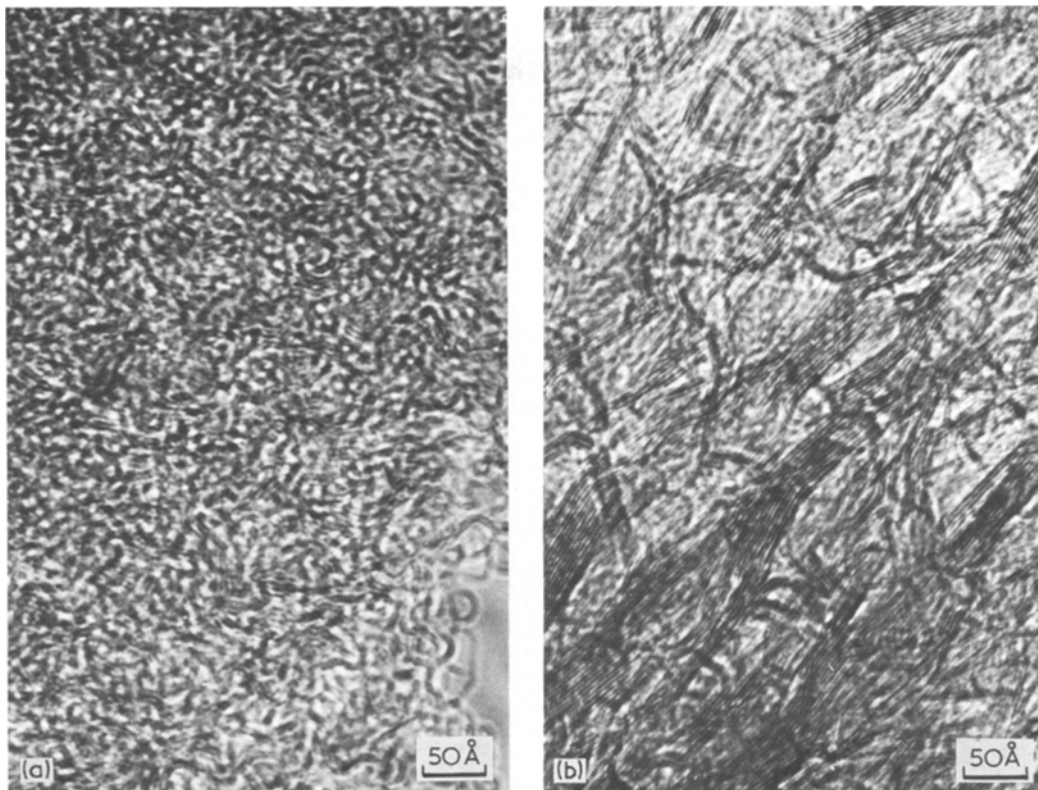


**Figure 11** Phase contrast electron micrograph (axial illumination) of (a) 1000° C glassy carbon fibre, (b) stretch-graphitized fibre, 60% extended at 2700° C. Fibre axes parallel to plane of micrographs.

stitial atoms which may be present in these “hard”, polymer carbons (i.e. partial graphitization), as well as a disentangling and dewrinkling of the microfibrils leading to their preferential orientation about the tensile (axial) direction. These microstructural changes are illustrated for the petroleum-pitch-based carbon fibres by the high resolution electron micrographs\* in Fig. 11, which show this “recrystallization” (ordering) and alignment of the carbon layer plane units. Further evidence for these microstructural effects of stretch-graphitization on glassy carbon fibres, and fibres from rayon precursor, has been obtained from electron and X-ray diffraction studies [9, 10]. Also the ease of plastically deforming any carbon fibre depends on its potential for structural ordering since, for example, it is difficult to extend those fibres which have already been partly annealed by prior heat-treatment unless even higher temperatures are used during stretching [16, 23]. Non steady-state creep is possible in high temperature treated glassy carbons [14], but it appears that only when the ordering (partial graphitization) and ribbon straightening processes

operate together are the fast deformation rates, characteristic of stretch-graphitization, possible.

The apparent activation energy of  $\sim 350 \text{ kcal mol}^{-1}$  reported [14] for tensile creep, between 2500 to 2900°C, in bulk glassy carbon (preheated to  $\sim 3000^\circ \text{C}$ ) is  $\sim 100 \text{ kcal mol}^{-1}$  greater than those of other high temperature processes in carbonaceous materials, which correspond approximately to theoretical and experimental values for point defect diffusion activation energies in these solids [15]. It has been suggested that this discrepancy may be partly due to the temperature dependence of the glassy carbon shear modulus [23] but in view of the creep data for other carbonaceous solids listed in Table II this argument [23] would also apply to the creep activation energies obtained in these materials. An alternative explanation of the relatively high  $\Delta H$  value for glassy carbon is that it may be characteristic of a ribbon deformation process unique to the randomly arranged microfibrillar substructure of glassy carbons which is rate-controlling under high stress conditions ( $> 6000 \text{ psi}$  in the creep study on partly ordered, “pre-annealed” glassy carbon [14]). On this basis

\* Electron micrographs kindly provided by Drs D. Crawford and D. J. Johnson, University of Leeds.

the presently obtained  $\Delta H$  value for stretch-graphitization can be rationalised by postulating that a mutual interaction exists between the simultaneously operating ribbon straightening and point defect annealing processes such that the activation energy associated with the ribbon deformation process is reduced in the stretch-graphitization of the much more disordered glassy carbon fibres. Since no systematic variation of the present  $\Delta H$  value was observed with temperature this proposed interaction would be essentially constant over the temperature range studied.

The observed strong stress dependence of the strain-rate rules out a rate-limiting Nabarro–Herring mechanism even if this could be considered feasible for the high experimental deformation rates. Again because of both the large stress exponent obtained and the doubtful existence of dislocations in the microstructure of polymer carbons, especially glassy carbon, the controlling operation of the usual high temperature dislocation mechanisms in the fibre stretch-graphitization are considered unlikely.

The present data from strain-rate change experiments apparently indicate an exponential dependence of creep rate on stress over the ranges studied, as is found for some metals and poly-

meric solids. As shown in Fig. 12 the data set from Fig. 7 which extends over the largest strain-rate range, but which is otherwise typical, conforms well to a linear relationship between log strain-rate and stress. From such plots the apparent activation volume,  $\Delta V$ , for the stretch-graphitization process may be calculated from the equation

$$\Delta V = 2kT(d \ln \dot{\epsilon} / d\sigma)_T$$

where  $k$  is Boltzmann's constant. The mean value of  $\Delta V$  obtained from all experimental data is approximately  $4000 \text{ \AA}^3$ , consistent with the observed high stress exponent. Such a large apparent activation volume suggests that the activated step in stretch-graphitization may indeed be associated with molecular-, rather than atomic-, scale processes.

The present high  $\Delta V$  value is of the same order ( $\leq$  twice as large) as those found for yielding and high stress creep in some glassy organic polymers, e.g. polystyrene [24], epoxy resins [25], polycarbonate [26], etc. where  $\Delta V$  is regarded as a measure of the volume of the activated molecular unit involved in the diffusion process [25]. Distortional yielding of linear (and lightly cross-linked [27]) amorphous polymers in their glassy

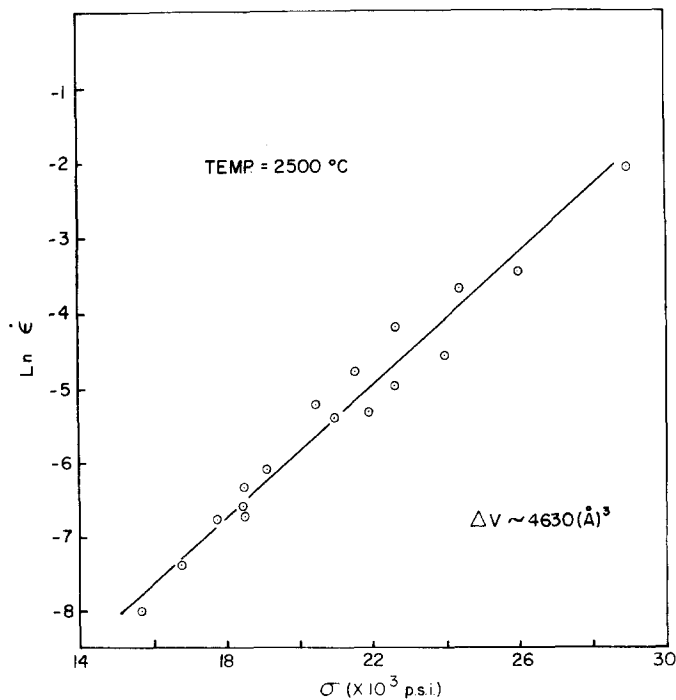


Figure 12 Natural logarithm of strain-rate versus fibre stress for the data set which extends over largest strain-rate range, showing linear relationship.

state is a viscoplastic process related to that inherent in the extension of amorphous polymer fibres by cold-drawing [25–28] which can proceed either by necking or by affine deformation above their glass transition temperatures. Axial alignment of the randomly oriented macromolecules takes place by the activated, stress-biased, reorientation of short chain segments [25–29], sometimes involving the co-operative movement of several molecules [28]. The progressive structural ordering and alignment of randomly oriented, interwoven microfibrils (with consequent work-hardening) which results from stretch-graphitization of glassy carbon fibres phenomenologically resembles the microstructural changes which occur on extending amorphous polymer fibres. In view of this and the approximate correspondence observed between experimental activation volumes it is suggested that stretch-graphitization may be considered analogous to the affine drawing of amorphous polymer fibres and that the basic mechanism involves the incremental movement of microfibril segments in the glassy carbon structure.

While recognizing the differences between amorphous organic polymers and glassy carbons several further apparent parallels in their microstructure and plastic deformation behaviour are noted briefly. Firstly, at the molecular level, the granular ordered regions,  $\sim 50 \text{ \AA}$  in diameter, observed in such polymers [30] plausibly resemble the “crystallites” similarly detected in glassy carbons [1, 2, 10] which, by using phase contrast electron microscopy [2], have been identified as the less distorted layer-plane packets of the random microfibrillar substructure (see Fig. 11a). The microporosity of glassy carbons also bears analogy with the excess free volume concentrated in intergrain regions in amorphous polymers which, it has been posed [30], facilitates plasticity in these materials. That the microfibril rearrangement involved in the plastic deformation of polymer carbons is likely accommodated by their porosity has been recognized for some time [31].

Lastly, oscillating flow stresses exhibiting sawtooth waveforms not unlike those observed in the stretch-graphitization experiments are sometimes obtained during the drawing of amorphous [32] (and semi-crystalline [33]) organic polymer fibres. However, when large, such oscillations are associated with intermittent void formation in the polymer fibres caused by hydrostatic stresses in

the cold-drawing neck region [33]. It is not known if such features are present in stretch-graphitized glassy carbon fibres (at frequencies  $> 100 \text{ in.}^{-1}$ ) but since present oscillations were monitored on fibres deforming in an affine manner their origin may be quite different from the polymer case. In stretch-graphitization the small oscillations possibly arise from the operation of sequential exhaustion processes where local resources of fibre plasticity are used up but, because of their observed frequency, they do not seem to be related to molecular scale processes and further study is needed before they can be properly explained.

## 5. Summary and conclusions

The main conclusions which arise from this study are summarized as follows: The continuous stretch-graphitization of isotropic glassy carbon fibres is a dynamic, steady-state plastic extension process in which the fibres, deforming in an affine manner essentially at constant volume, sequentially along their length become more ordered and anisotropic as their microfibrillar substructure becomes preferentially oriented in the stretching direction. The characteristic parameters of stretch-graphitization, i.e. the apparent activation energy and activation volume, are consistent with the simultaneous operation of atomic diffusion and a molecular-scale process, which latter is rate-limiting and is probably associated with the sequential reorientation of microfibril segments.

## Acknowledgements

Thanks are expressed to Mr G. Fraser for assistance with some of the experimental work and acknowledgement is made to Dr R. H. Bentall, formerly of this laboratory, who initiated the fibre quenching technique. The financial support of the National Research Council of Canada is recorded with gratitude.

## References

1. S. YAMADA, D.C.I.C. Report 68-2 (1968) U.S. Defence Documentation Centre, Virginia.
2. G. M. JENKINS, K. KAWAMURA and L. L. BAN, *Proc. Roy. Soc. (London)* A327 (1972) 501.
3. S. OTANI, *Carbon* 4 (1966) 425.
4. H. M. HAWTHORNE, C. BAKER, R. H. BENTALL and K. R. LINGER, *Nature* 227 (1970) 946 (also Can. Patent 903444, June 1972).
5. S. OTANI, Y. KOBUKO and T. KOITABASHI, *Bull. Chem. Soc. Japan* 43 (1970) 3291.
6. R. BACON, A. A. PALLOZZI and S. E. SLOSARIK, Proceedings of the S.P.I. 21st Technical Conference (1966) Section 8E.

7. J. W. JOHNSON, J. R. MARJORAM and P. G. ROSE, *Nature* **221** (1969) 357.
8. W. JOHNSON, Proceedings of the 3rd Conference Industrial Carbons and Graphite, S.C.I., London (1970) p. 447.
9. R. BACON, "Chemistry and Physics of Carbon" Vol. 9, edited P. L. Walker Jun. (Marcel Dekker, New York, 1973) p. 1-102.
10. H. M. HAWTHORNE, Proceedings of the 1st International Carbon Fibre Conference, London (1971) (Plastics & Polymers Conf. Supplement no. 5) p. 81.
11. S. OTANI, S. WATANABE, H. OGINO, K. IJIMA and T. KOITABASHI, *Bull. Chem. Soc. Japan* **45** (1972) 3701.
12. W. N. REYNOLDS, "Physical Properties of Graphite" (Elsevier, London, 1968).
13. E. G. ZUKAS and W. V. GREEN, *Carbon* **6** (1968) 101.
14. D. B. FISCHBACH, *ibid* **9** (1971) 193.
15. *Idem*, "Chemistry and Physics of Carbon" Vol. 7, edited by P. L. Walker Jun. (Marcel Dekker, New York, 1971).
16. H. M. HAWTHORNE, unpublished results.
17. A. A. KHOMENKO, Yu. E. SMIRNOV, V. P. SOSEDOV and V. L. KASATOCHKIN, *Dokl. Akad. Nauk. SSSR* **206** (1972) 1112 (*Sov. Phys. Dokl.* **17** (1973) 956).
18. C. D. WIGNALL and C. J. PINGS, *Carbon* **12** (1974) 51.
19. M. NAKAMIZO, R. KAMMERECK and P. L. WALKER JUN., *ibid* **12** (1974) 259.
20. A. G. WHITTAKER and B. TOOPER, *J. Amer. Ceram. Soc.* **57** (1974) 443.
21. R. R. SAXENA and R. H. BRAGG, *Carbon* **12** (1974) 211.
22. A. FOURDEUX, C. HÉRINCKX, R. PERRET and W. RULAND, *Compt. Rend.* **269C** (1969) 1597.
23. T. G. LANGDON, *Nature Phys. Sci.* **236** (1972) 60.
24. F. BUECHE, "Physical Properties of Polymers" (Interscience, New York, 1962).
25. O. ISHAI, *J. Appl. Polymer. Sci.* **11** (1967) 1863.
26. R. E. ROBERTSON, *ibid* **7** (1963) 443.
27. O. ISHAI, *ibid* **11** (1967) 963.
28. A. S. ARGON, *Phil. Mag.* **28** (1973) 839.
29. R. E. ROBERTSON, *J. Chem. Phys.* **44** (1966) 3950.
30. G. S. Y. YEH, *J. Macromol. Sci.* **B6** (1972) 465.
31. R. BACON and W. H. SMITH, Proceedings of the 2nd Conference on Industrial Carbons and Graphite, S.C.I., London (1965) p. 1.
32. H. LUDEWIG, "Polyester Fibres - Chemistry & Technology" (Interscience, New York, 1971).
33. D. C. HOOKWAY, *J. Text. Inst.* **49** (1958) 292.
34. D. B. FISCHBACH and W. V. KOTLENSKY, *Electrochem. Tech.* **5** (1967) 207.
35. E. G. ZUKAS and W. V. GREEN, *Carbon* **10** (1972) 519.
36. H. N. MURTY, D. L. BIEDERMAN and E. A. HEINTZ, *ibid* **7** (1969) 667.
37. B. GRANOFF, *ibid* **12** (1974) 405.

Received 23 April and accepted 27 May 1975.